Hindawi Publishing Corporation
Journal of Nanomaterials
Volume 2014, Article ID 582913, 11 pages
http://dx.doi.org/10.1155/2014/582913

Research Article

The Effect of Chemical and High-Pressure Homogenization Treatment Conditions on the Morphology of Cellulose Nanoparticles

Suxia Ren,[1] Xiuxuan Sun,[2] Tingzhou Lei,[1] and Qinglin Wu[2]

[1] *Key Biomass Energy Laboratory of Henan Province, Zhengzhou, Henan 450008, China*
[2] *School of Renewable Natural Resources, Louisiana State University Agricultural Center, Baton Rouge, LA 70803, USA*

Correspondence should be addressed to Tingzhou Lei; leitingzhou@163.com and Qinglin Wu; qwu@agcenter.lsu.edu

Received 22 July 2014; Revised 10 September 2014; Accepted 12 September 2014; Published 19 October 2014

Academic Editor: Antonios Kelarakis

Cellulose nanoparticles were fabricated from microcrystalline cellulose (MCC) through combined acid hydrolysis with sulfuric and hydrochloric acids and high-pressure homogenization. The effect of acid type, acid-to-MCC ratio, reaction time, and numbers of high-pressure homogenization passes on morphology and thermal stability of the nanoparticles was studied. An aggressive acid hydrolysis was shown to lead to rod-like cellulose nanocrystals with diameter about 10 nm and lengths in the range of 50–200 nm. Increased acid-to-MCC ratio and number of homogenization treatments reduced the dimension of the nanocrystals produced. Weak acid hydrolysis treatment led to a network of cellulose nanofiber bundles having diameters in the range of 20–100 nm and lengths of a few thousands of nanometers. The high-pressure homogenization treatment helped separate the nanofiber bundles. The thermal degradation behaviors characterized by thermogravimetric analysis at nitrogen atmosphere indicated that the degradation of cellulose nanocrystals from sulfuric acid hydrolysis started at a lower temperature and had two remarkable pyrolysis processes. The thermal stability of cellulose nanofibers produced from hydrochloric acid hydrolysis improved significantly.

1. Introduction

As the most abundant and renewable biopolymer provided by nature, cellulose is attracting a lot of research effort in many scientific disciplines and continues to be a subject of intense studies for its utilization as functional materials. Cellulose is a linear polymer consisting of D-anhydroglucose units joined together by β-1, 4-glycosidic linkages that gives rise to various crystalline domain formations [1]. These crystalline domains possess very high strength and modulus, approximately on the order or great than a comparable structural steel sample [1, 2]. The crystal structures of celluloses are known as cellulose I and cellulose II, respectively. The smallest discernible building block of cellulose I is a bundle of parallel glucan chains, typically with a square or close-to-square cross section known as a cellulose I fibril [2]. The strong mutual packing of fibrils in a fibril aggregate makes them difficult to disintegrate. Generally, there are four methods commonly used to isolate bundles of cellulose fibers, that is, acid hydrolysis, enzymatic hydrolysis, mechanical shearing, and enzymatic hydrolysis combined with mechanical shearing and high-pressure homogenization [3–5].

Treatment with sufficient strong acid can effectively break down the amorphous cellulose, thus liberating cellulosic nanosized crystals [4, 6]. Strong acidic conditions combined with sonication lead to aggressive hydrolysis to attack the noncrystalline fractions. This results in mainly low aspect ratio cellulose I fibril aggregates and fibrils, which are also denoted as whiskers [3, 7, 8]. Analogous to the acid hydrolysis treatment described above, cellulose enzymes can be used to attack on the amorphous regions of cellulosic substrates. Henriksson et al. [9] reported that such treatment made it easier to separate the material into microfibrillated cellulose. Janardhnan and Sain [10] found that enzymatic treatment led to a smaller particle size range of cellulose, following high-shear refining. Mechanical shearing method eliminates the hydrolysis step altogether and solely imposes high shearing forces for disintegration. This yields a highly entangled

Table 1: Summary of different treatment conditions on microcrystalline cellulose used in the study.

Sample ID	Acid type and concentration	Acid-to-MCC ratio (mL/g)	Temperature (°C)	Treating time (h)	Number of high-pressure treatment
A	64 wt% H_2SO_4	3.50	45	1	20
B	64 wt% H_2SO_4	8.75	45	1	10
C	64 wt% H_2SO_4	14.0	45	3	35
D	64 wt% H_2SO_4	17.5	45	3	35
E	37.5 wt% HCl	17.5	45	1	25
F	37.5 wt% HCl	17.5	45	3	35

network, which typically consists of elements having a wide size distribution down to nanoscale [11–13]. The resulting material has been denoted microfibrillated cellulose (MFC), originally introduced by Turbak et al. [11] and Herrick et al. [12]. Pääkko et al. [14] demonstrated that a combination of high-pressure shear forces and mild enzymatic hydrolysis constitutes a new and efficient method to prepare MFC with a well-controlled diameter in the nanometer range and to maintain high aspect ratio, in contrast to acid hydrolysis. In particular, it is demonstrated that strong aqueous gels with highly tunable storage modulus can be obtained, which suggests application of MFC to reinforce multicomponent mixtures. Other techniques in isolating cellulose nanoparticles include the use of TEMPO-mediated oxidation and ionic liquids. For example, in a more recent study, regenerated cellulose nanoparticles (RCNs) including both elongated fiber and spherical structures were prepared from microcrystalline cellulose (MCC) and cotton using 1-butyl-3-methylimidazolium chloride followed by high-pressure homogenization [15]. The crystalline structure of RCNs was cellulose II in contrast to the cellulose I form of the starting materials. Also, the RCNs had decreased crystallinity and crystallite size. The dimensions of the various RCNs were all well fitted with an asymmetrical log-normal distribution function. The RCN had a two-step thermal pyrolysis, different from raw MCC and cotton that had a one-step process.

This work was intended to provide a comparative study for manufacturing cellulose nanoparticles in a more economical and environmentally friendly manner. This approach was based on acid hydrolysis combined with high-pressure homogenization. The specific objectives were to study the effect of acid type, acid-to-MCC ratio, reaction time, and number of high-pressure homogenization treatments on the resulting nanofibers and nanocrystals. The structure of the cellulose nanofibers and cellulose nanocrystals was investigated using transmission electron microscopy (TEM). The thermal degradation behaviors of the manufactured materials were characterized using thermogravimetric analysis (TGA).

2. Experimental

2.1. Material. Microcrystalline cellulose (MCC, Avicel FD-100, FMC Biopolymer, Philadelphia, PA) was selected as raw material for producing the cellulose nanoparticles. The MCC are cellulose agglomerates (i.e., purified cellulose around 30 μm in length). These large size structures are formed by the strong hydrogen bonding between microfibrils and are the typical characteristic of this cellulose powder [16, 17]. Sulfuric acid (95–98 wt%) and hydrochloric acid (36.5–38.0 wt%) were obtained from VMR (West Chester, PA). All water used was distilled water.

2.2. Preparation of Cellulose Nanofibers/Nanocrystals

2.2.1. Chemical Treatment. Acid hydrolysis was performed with six experimental conditions (Table 1). Four sulfuric acid and two hydrochloric acid treatments were used.

MCC was subjected to sulfuric acid and hydrochloric acid hydrolysis at 45°C for 1–3 h with different acid-to-MCC ratios. Immediately following hydrolysis, suspensions were diluted fivefold to stop the reaction. The suspensions were then centrifuged at 12,000 rpm for 10 min (Sorvall RC-5B Refrigerated Superspeed Centrifuge, DuPont Instrument, Newtown, Connecticut) and washed with distilled water for 5 times, and the particles were separated from the suspension by centrifuging after each washing. The precipitate was then placed in regenerated cellulose dialysis tubing (Fisher Scientific, Pittsburgh, PA) having a molecular weight cutoff of 12,000–14,000 and dialyzed against distilled water for several days until the water pH reached a value of 7.0.

2.2.2. Mechanical Treatment. To further reduce the size of the cellulose nanoparticles, mechanical treatment was applied to the chemically treated samples. The suspensions were passed through a high-pressure homogenizer (Microfluidizer M-110P, Microfluidics Corp., Westwood, MA), equipped with a pair of Z-shaped interaction chambers (one 200 μm ceramic and one 87 μm diamond) for the designated numbers of passes. The operating pressure was 207 MPa. Sample suspensions after each pass through the high-pressure homogenizer were collected for analysis.

2.3. Characterization of Cellulose Nanofibers/Nanocrystals

2.3.1. Morphology and Size. Morphology of chemically and mechanically treated cellulose nanofibers and cellulose nanocrystals were characterized by transmission electron microscopy (TEM) (JEOL USA Inc., Peabody, MA, USA), using an acceleration voltage of 80 kV. A drop (5 μL) of a dilute suspension of cellulose nanoparticles was deposited on a carbon-coated grid and stained by uranyl acetate to improve the contrast. The distribution of the nanoparticles dimensions was obtained from the analysis of these images. The TEM

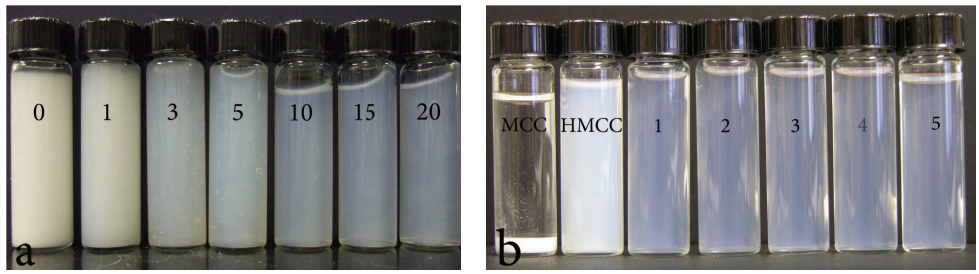

(a) (b)

Figure 1: (a) Photograph of acid-hydrolyzed MCC (Sample A) and high-pressure homogenizer treated cellulose nanocrystals (1, 3, 5, 10, 15, and 20 passes through the homogenizer); (b) photograph of microcrystalline cellulose (MCC), acid-hydrolyzed MCC (Sample D), and high-pressure homogenizer treated cellulose nanocrystals (1 through 5 passes through the homogenizer).

micrographs were loaded to the Adobe Photoshop software and over fifty particles were measured using the ruler tool in each image.

2.3.2. Thermal Analysis. Thermogravimetric analysis (TGA) measurements of manufactured nanocrystals and nanofibers were carried out with a TGA Q50 (TA Instrument, New Castle, DE). The samples were heated up from 30 to 550°C at a heating rate of 5°C/min under a nitrogen flow rate of 50 mL·min^{-1}. Sample weights were between 3 mg and 5 mg for each run. TG and derivative TG (DTG) data were obtained for each sample set, from which thermal degradation parameters were extracted.

3. Results and Discussion

3.1. Sulfuric Acid Hydrolysis

Suspension Appearance. Figure 1(a) shows a photograph of the suspensions from acid-hydrolyzed MCC (Sample A, subjected to 1 h sulfuric acid hydrolysis using an acid-to-MCC ratio of 3.5 mL/g) and high-pressure homogenized materials from sample A, which passed through the homogenizer 1, 3, 5, 10, 15, and 20 times, respectively. As shown in Figure 1(a), the suspension of the acid-hydrolyzed cellulose appeared to be milk white, and those mechanical treated samples gradually formed blue transparent suspension due to the gradually minimized size of the cellulose nanoparticles. Figure 1(b) shows a photograph of Sample D (subjected to 3 h sulfuric acid hydrolysis using an acid-to-MCC ratio of 17.5 mL/g) and high-pressure homogenized materials from Sample D, which passed through the homogenizer 1, 3, and 5 times, respectively. As shown in Figure 1(b), the large agglomerates of MCC precipitated at the bottom in a short time after being added into water. The acid-hydrolyzed cellulose formed stable opalescent suspension in water. By homogenizing these acid-hydrolyzed cellulose nanoparticles under high pressure, the size of the particles was further minimized, and individual nanocrystals were formed. These nanocrystals dispersed in water without visible aggregation and formed light blue transparent suspension in water as shown by the samples labeled "1" through "5" (Figure 1(b)).

Morphology and Size. Figure 2 shows the TEM images of the cellulose nanoparticles (Sample A). It can be seen that an acid-to-MCC a too low acid-to-MCC weight ratio only yielded large micron-scale, irregular-shaped, undispersable fiber networks, which aggregated in water even after 15 passes through the homogenization process (Figure 2(f)).

Figure 3 shows the TEM images of Sample B ((a): subjected to 1 h sulfuric acid hydrolysis using an acid-to-MCC ratio of 8.75 mL/g and (b), (c), and (d): cellulose nanoparticles with high-pressure homogenization treatment of 3, 5, and 10 passes, resp.). The samples shown in Figures 3(a) and 3(b) show irregular fiber bundles. After five passes (samples shown in Figures 3(c) and 3(d)), rod-form crystals appeared. These nanocrystals are about 10 nm in diameter and 100–200 nm in length. The distribution of nanocrystal dimensions was obtained from the analysis of these images (Figure 3(e)) and the data is shown in Figure 3(e). The particle length distribution spread over a range of 60 nm to 380 nm for the sample shown in Figure 3(a). As the homogenization cycle increased, the distribution narrowed significantly and shifted toward left (smaller length side).

The mean crystal size data is summarized in Table 2. The four samples from Sample B show a decreased mean crystal length and a similar crystal diameter. The average crystal length was 186 ± 66 nm for Sample B and 141 ± 28 nm, 121 ± 30 nm, 124 ± 48 nm for high-pressure homogenizer treated cellulose nanocrystals after being processed through the homogenizer 3, 5, and 10 passes, respectively. The data illustrated that the high-pressure homogenizer treatments effectively reduced the length of the cellulose crystals. The aspect ratio of the crystals was found to be about 13–16.

Figures 4(a), 4(b), 4(c), and 4(d) show the TEM images of Sample C (subjected to 3 h sulfuric acid hydrolysis using an acid-to-MCC ratio of 14 mL/g) and cellulose nanocrystals with high-pressure homogenization treatment for 1, 3, 5, and 20 times, respectively. Rod-shape crystals were obtained directly after the acid hydrolysis. These nanocrystals were about 10 nm in diameter and 90–150 nm in length. The distribution of nanocrystal dimensions obtained from the analysis

Table 2: Effect of treatment conditions on the size of cellulose nanocrystals.

Sample	Variables	Treatment cycle			
		0	3	5	10
B	Length, L/nm	186 ± 96	141 ± 28	121 ± 30	124 ± 48
	Diameter, D/nm	11.6 ± 2.8	9.0 ± 1.4	9.0 ± 1.6	9.0 ± 2.0
	Axial ratio, L/D	16	15.7	13.4	13.7
		0	1	3	20
C	Length, L/nm	149 ± 54	145 ± 47	118 ± 66	93 ± 26
	Diameter, D/nm	9.4 ± 2.2	11.5 ± 1.9	10 ± 2.6	8.9 ± 1.8
	Axial ratio, L/D	15.8	12.6	11.8	10.5
		0	1	3	5
D	Length, L/nm	124 ± 28	112 ± 25	94 ± 22	62 ± 26
	Diameter, D/nm	7.9 ± 1.6	7.7 ± 1.5	9.5 ± 1.8	8.7 ± 1.2
	Axial ratio, L/D	15.7	14.5	9.9	7.2

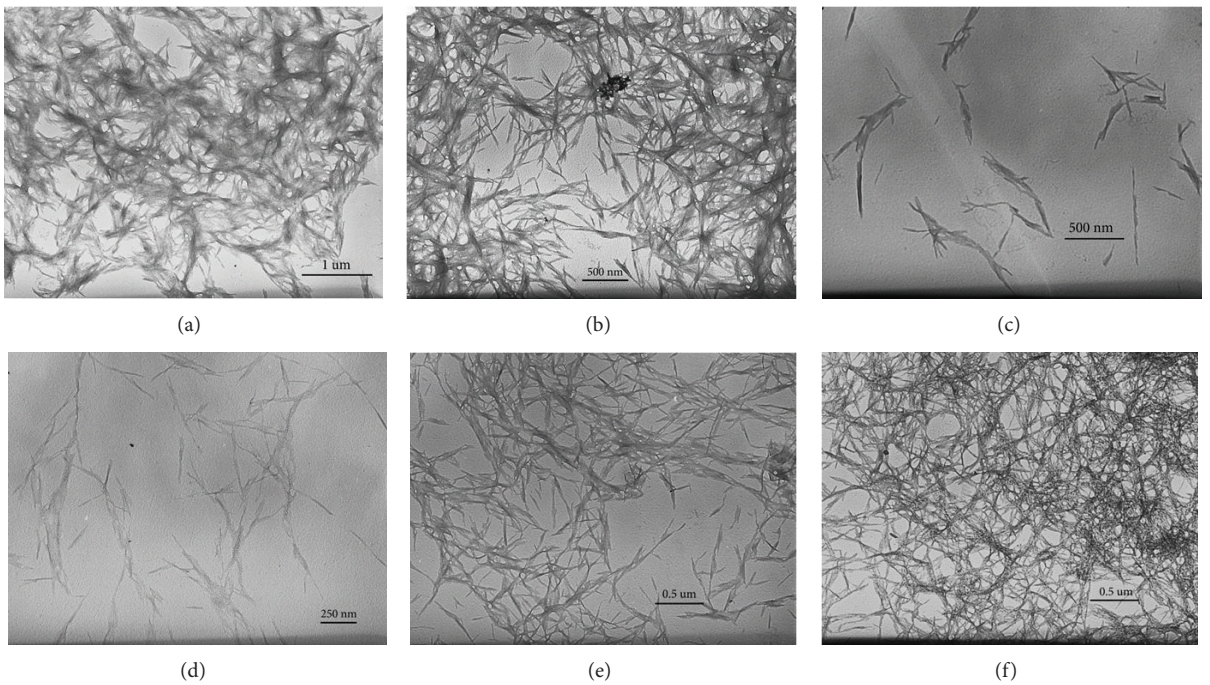

Figure 2: Transmission electron microscopy (TEM) images of (a) for acid-hydrolyzed cellulose nanoparticles (Sample A) and (b), (c), (d), (e), and (f) for high-pressure homogenizer treated cellulose nanoparticles with 1, 3, 5, 10, and 15 passes through the homogenizer, respectively.

of these images (Figure 4(e)) shows a gradually narrowed length range and left-shift (i.e., toward the smaller crystal length side) as the homogenization cycle increased, similar to that of Sample B. The distribution was generally narrower, less polydispersed, and attributable to the higher acid-to-MCC ratio. The mean crystal size data shown in Table 2 indicates a smaller mean particle length of Sample C compared to that of Sample B. The four samples show a decreased crystal length and a similar crystal diameter. The average crystal length was 149 ± 54 nm, 145 ± 47 nm, 118 ± 66 nm, 93 ± 26 nm, and 100 ± 31 nm for high-pressure homogenizer treated cellulose nanocrystals after being processed through the homogenizer 1, 3, 5, 20, and 35 passes, respectively. The data illustrated that the high-pressure homogenizer treatments effectively reduced the length of the cellulose crystals. The aspect ratio of the crystals was found to be about 10–16.

Figures 5(a), 5(b), 5(c), and 5(d) show the TEM images of Sample D (subjected to 3 h sulfuric acid hydrolysis using an acid-to-MCC ratio of 17.5 mL/g) and cellulose nanocrystals with high-pressure homogenization treatment for 1, 3, and 5 times, respectively. Similar to Sample C, rod-shape crystals were obtained directly from the acid-hydrolyzed samples. These nanocrystals are 7–10 nm in diameter and 60–120 nm in length. The distribution of nanocrystal dimensions is shown in Figure 5(e) with mean size data summarized in Table 2. The samples show a similar crystal length polydispersity as Sample C. The four samples show a decreased crystal length and a similar crystal diameter (Table 2). The average

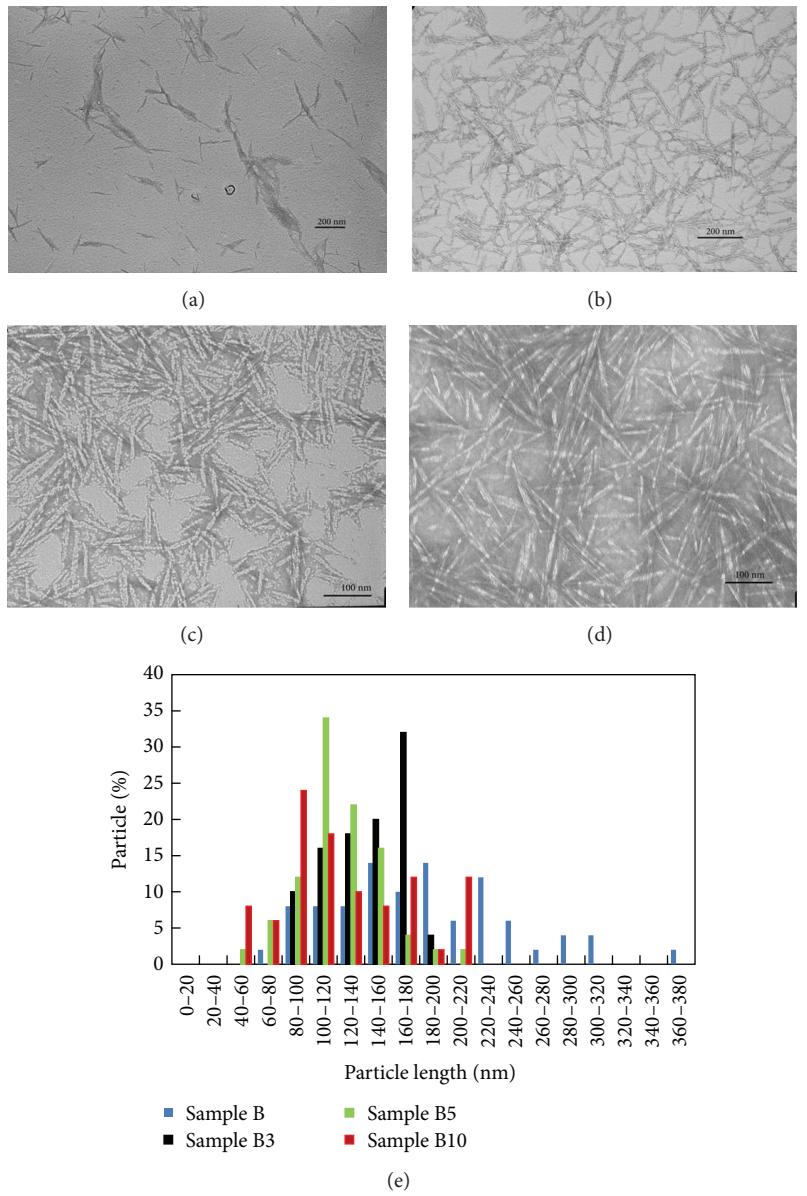

FIGURE 3: Transmission electron microscopy images of (a) for acid-hydrolyzed cellulose crystal (Sample B); and (b), (c), and (d) for high-pressure homogenizer treated cellulose crystals at 3, 5, and 10 passes through the homogenizer, respectively, and their length distribution.

crystal length was 124 ± 28 nm for the acid-hydrolyzed MCC (HMCC) and 112 ± 25 nm, 94 ± 26 nm, 62 ± 22 nm for high-pressure homogenizer treated cellulose nanocrystals after being processed through the homogenizer 1, 3, and 5 passes, respectively. The aspect ratio of the crystals was found to be about 7–15, which is lower than those of Sample B and Sample C. The highest acid-to-MCC ratio led to the shortest cellulose nanocrystals, which is about 100 nm in length, and the high-pressure homogenization helped reduce the length to two-thirds of the acid-hydrolyzed samples.

Thermal Degradation Properties. The TG and DTG curves of MCC and sulfuric acid hydrolyzed MCCs are shown in Figure 6. For MCC, a broad DTG peak centered at 50°C was found (not shown), corresponding to a weight loss of 2.2%, which was due to the evaporation of absorbed water. The sharp DTG peak centered at 328.5°C was due to the concurrent cellulose degradation processes including depolymerization, dehydration, and decomposition of glycosyl units followed by the formation of a charred residue. The degradation behavior of sulfuric acid hydrolyzed cellulose crystals showed a significant difference from that of unhydrolyzed MCC. The degradation of cellulose nanoparticles started at lower temperatures, following a two-stage degradation process in comparison with a single degradation process of MCC. The low-temperature process was between 150 and 250°C and the high-temperature process was between 300 and 400°C. The temperatures at the maximum degradation rates are, respectively, 328.58, 315.30, 309.39, 174.63, and 170.45°C for MCC and four hydrolyzed samples (i.e, A, B, C,

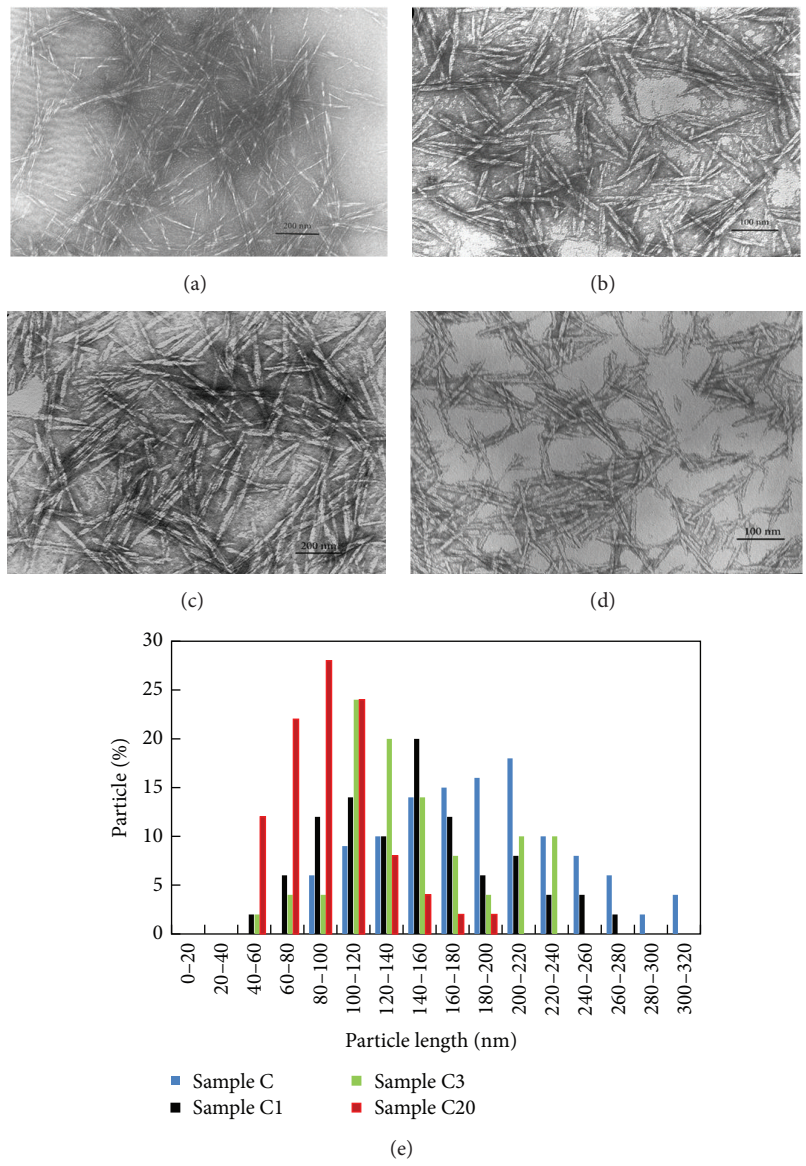

FIGURE 4: Transmission electron microscopy (TEM) images of (a) acid-hydrolyzed cellulose crystal (Sample C); (b), (c), and (d) for high-pressure homogenizer treated cellulose crystals after being processed through the homogenizer 1, 3, and 20 passes, respectively, and (e) their length distribution.

and D). Thus the temperatures shifted toward lower values, indicating decreased thermal stability of the nanoparticles, especially from Samples C and D.

Negative sulfate groups were introduced into the outer surface of cellulose nanoparticles during the hydrolysis process [18]. Han et al. [18] carried out a detailed study on the surface charge of several cellulose nanoparticles, using zeta potential in aqueous suspension and X-ray photoelectron spectroscopy (XPS) on freeze-dried particles. Results from both zeta potential and XPS measurements showed that cellulose I nanocrystals carried more $-O-SO_3^-$ groups on their surfaces. The study also showed that higher H_2SO_4 concentrations introduced more sulfate groups on the CNC surfaces during the acid hydrolysis process. Currently, no practical methods could be used to remove the sulfate group from the sulfuric acid-hydrolyzed material completely. The esterification levels of cellulose particles highly depend on hydrolysis time and acid concentrations.

The presence of the acid sulfate group decreased the thermal stability of the materials by dehydration reactions [19]. Thus, for cellulose nanocrystal samples with higher content acid sulfate groups, associated with the temperature range, it was considered that the lower temperature process was due to the primary pyrolysis of cellulose nanocrystals catalyzed by acid sulfate groups and that the higher temperature process was related to the slow charring process of the solid residue.

The residue weights for MCC and four hydrolyzed samples are, respectively, 9.40, 22.75, 31.29, 29.63, and 30.19%. The amount of char residue in acid hydrolyzed samples was, thus, markedly larger than these of the corresponding MCC

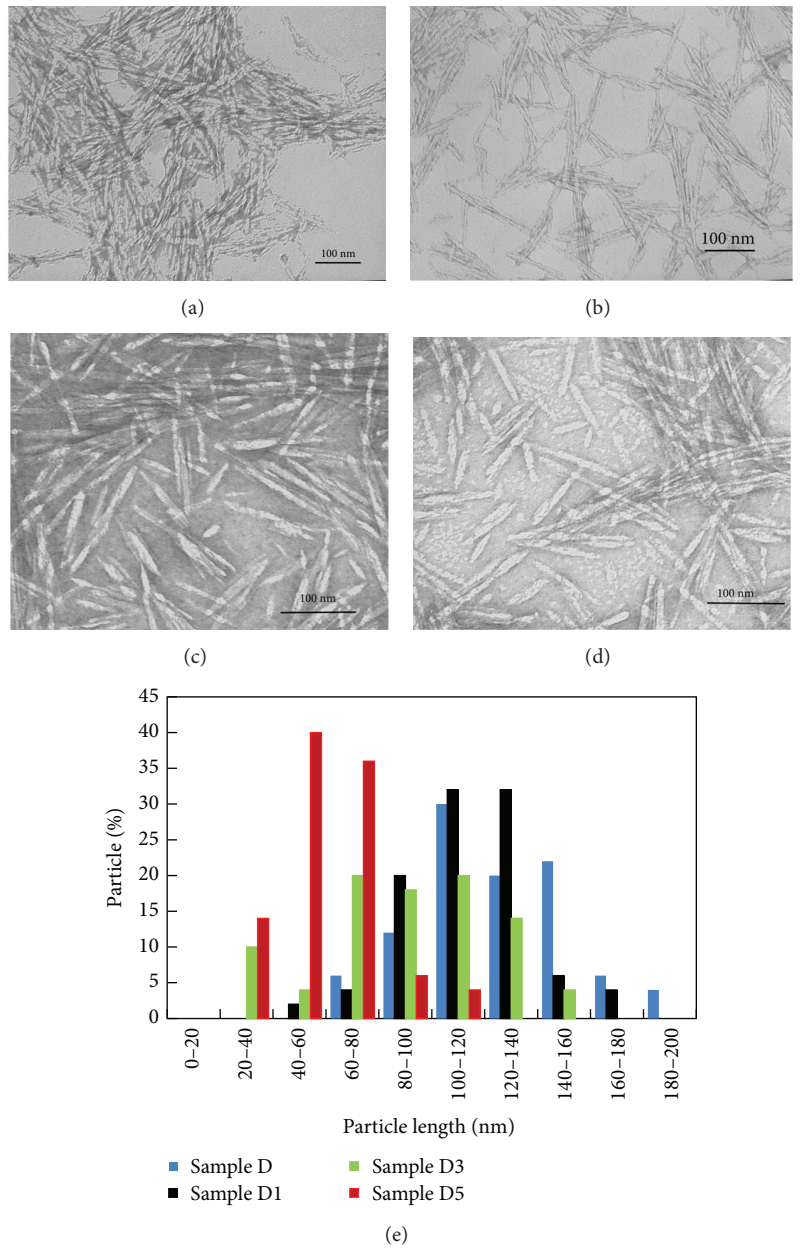

Figure 5: Transmission electron microscopy (TEM) images of (a) acid-hydrolyzed cellulose crystals (Sample D); (b), (c), and (d) for high-pressure homogenizer treated cellulose crystals after being processed through the homogenizer 1, 3, and 5 passes, respectively, and (e) distribution of particle length.

samples. The reason for this phenomenon was that cellulose nanocrystals had a great number of free end chains due to their small particle size. The end chains started decomposition at lower temperatures and, consequently, facilitated the increase of the char yield of HMCC. Similar degradation behaviors were observed and explained by other researchers [19, 20].

3.2. Hydrochloric Acid Hydrolysis

Morphology and Size. Figure 7 shows the TEM images of Sample E (subjected to 1 h hydrochloric acid hydrolysis using an acid-to-MCC ratio of 17.5 mL/g) and high-pressure homogenized materials from Sample E, which passed through the homogenizer 1, 3, 5, and 25 times, respectively. It is shown that hydrochloric acid hydrolysis only yielded several micron-size, undispersable fibers network. The network structure of the fiber bundles made it difficult to determine fiber length and width accurately.

Figure 8 shows the TEM images of Sample F (subjected to 3 h hydrochloric acid hydrolysis using an acid-to-MCC ratio of 17.5 mL/g) and high-pressure homogenized materials from Sample F, which passed through the homogenizer 5, 20, and 35 times, respectively. The increase in reaction time produced

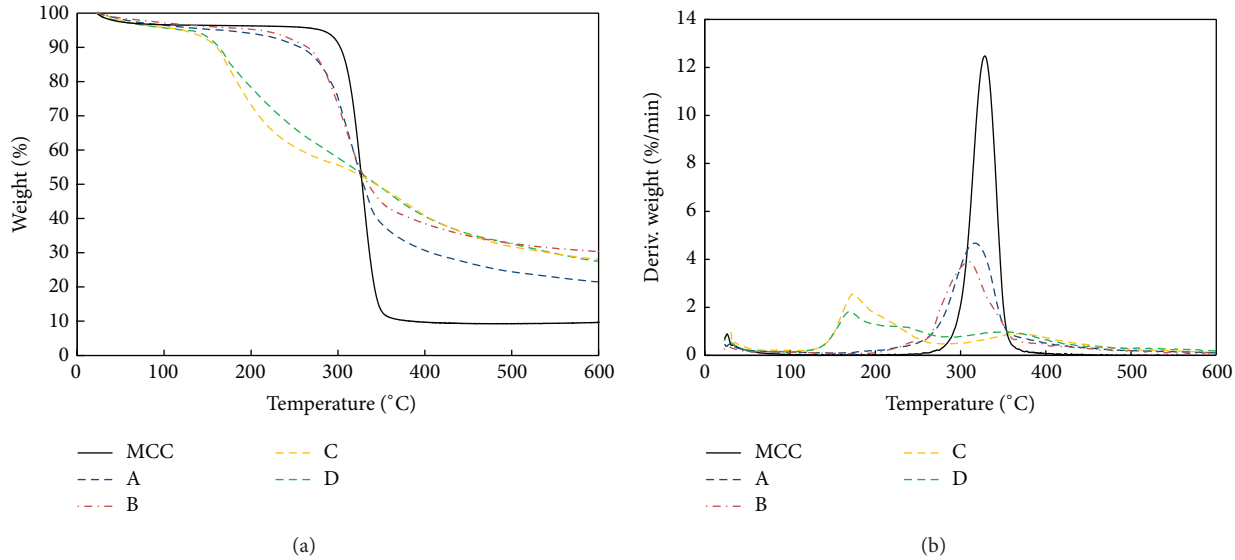

Figure 6: TGA (a) and DTG (b) curves of microcrystalline cellulose (MCC) and sulfuric acid-hydrolyzed MCC.

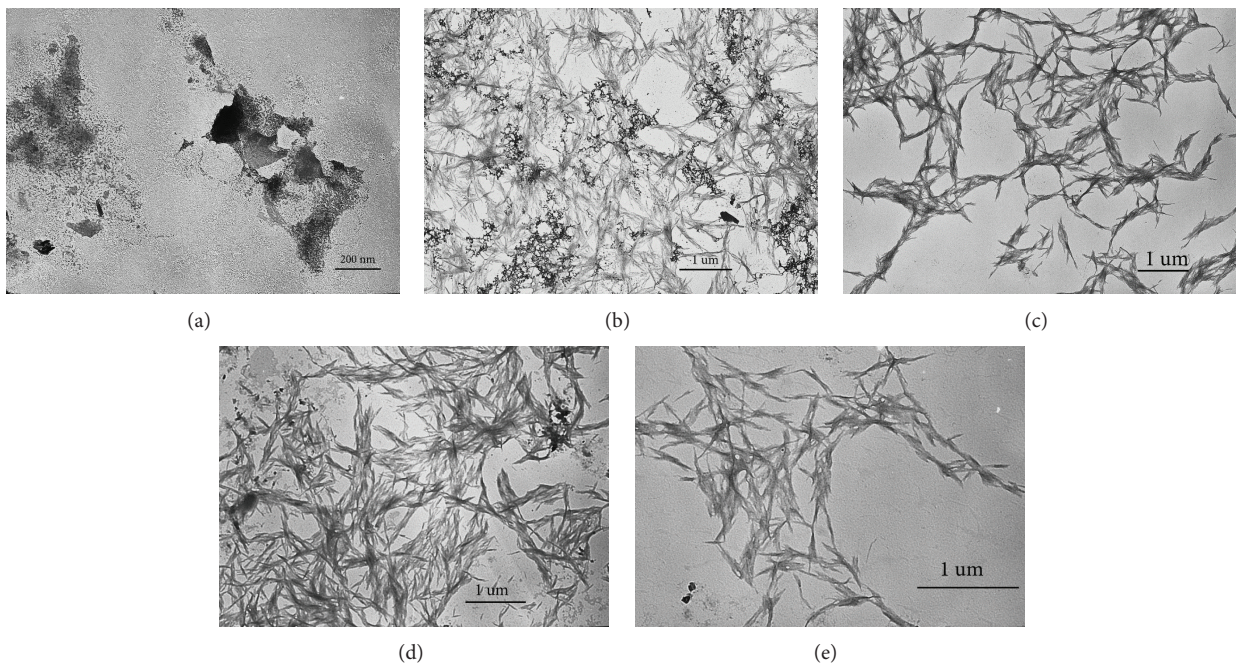

Figure 7: Transmission electron microscopy (TEM) images of (a) acid-hydrolyzed cellulose crystal (Sample E); (b), (c), (d), and (e) for high-pressure homogenizer treated cellulose crystals after being processed through the homogenizer 1, 3, 5, and 25 passes, respectively.

separated and shorter cellulose fibers (about 0.5 micron in length) compared with Sample E. However, those cellulose fibers were still much longer and more aggregated than those obtained from sulfuric acid hydrolysis at similar conditions.

Thermal Properties. The TG and DTG curves of MCC and cellulose fibers produced from hydrochloric acid hydrolysis are shown in Figure 9. A small DTG peak appeared in each of the two hydrolyzed samples. Thus, the degradation of the cellulose fibers was also a two-stage process, consisting of a low-temperature process between 200 and 250°C and a high-temperature process between 300 and 400°C. However, the high temperature stage dominated the whole degradation process, which was significantly different from that for sulfuric acid treatment materials. The temperatures at the maximum degradation rates are, respectively, 328.86, 350.77, and 317.27°C for MCC and two hydrolyzed samples (i.e., E and F). Thus, the thermal stability property of the original MCC materials was largely maintained or even improved in the hydrochloric acid treated materials. The results are in agreement with those reported by Yu et al. [21].

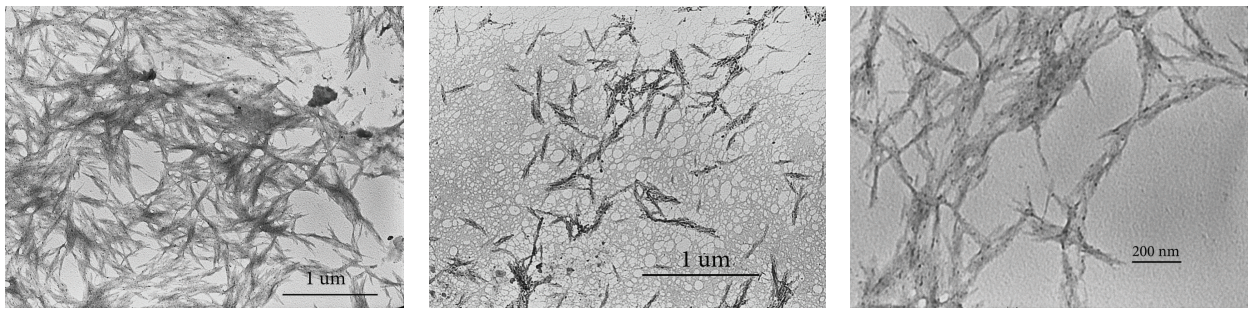

Figure 8: Transmission electron microscopy (TEM) images of (a), (b), and (c) for high-pressure homogenizer treated cellulose crystals (Sample F) at 5, 20, and 35 passes through the homogenizer, respectively.

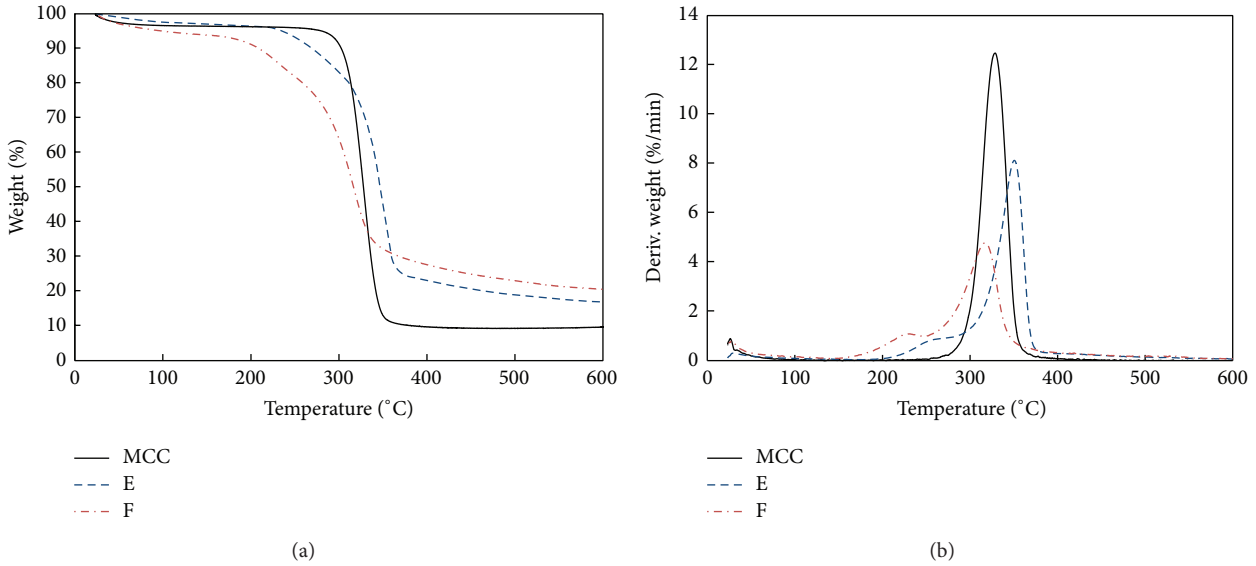

Figure 9: TGA (a) and DTG (b) curves of MCC and hydrochloric acid-hydrolyzed MCC samples.

The residue weights in the two hydrolyzed samples are, respectively, 17.70 and 21.44%, in comparison with 9.40% for the MCC samples. The amount of char residue in hydrochloric acid-hydrolyzed samples was larger than that of pure MCC, but it was lower than that of cellulose nanocrystals obtained from sulfuric acid hydrolysis.

3.3. Discussion. Past work on the crystalline structure of CNCs from acid hydrolysis has shown that the CNCs present three characteristic cellulose I reflections, corresponding to the $1\bar{1}0$, 110, and 200 crystallographic planes of the monoclinic cellulose I lattice [4, 16, 21]. Sulfuric acid hydrolysis of mercerized cellulosic fibers gave CNCs with cellulose II lattice [18, 22]. Compared with CNC I, cellulose II crystals are much shorter and had a better thermal stability due to fewer residual sulfate groups on the crystal surface [18].

Yu et al. [21], in an effort of developing a facile approach for extracting CNCs through hydrochloric acid hydrolysis of cellulose raw materials under hydrothermal conditions, showed that the CNCs produced through hydrochloric acid hydrolysis exhibited high thermal stability. In contrast, the degradation of CNCs from sulfuric acid hydrolysis exhibits poor thermal stability with the maximum degradation temperature (Tmax) of 250°C. The low thermal stability of the CNCs would prevent their further fabrications using several melt processing techniques such as injection molding, twin-screw compounding, and extrusion [23]. The low thermal stability of the CNCs was ascribed to the dehydration reaction induced by the residual sulfate groups (SO_4^{2-}) in the CNCs from sulfuric acid hydrolysis.

4. Conclusions

Cellulose nanofibers and nanocrystals were produced from microcrystalline cellulose through acid hydrolysis combined with high-pressure homogenization. Sulfuric acid and hydrochloric acid were utilized to conduct the acid hydrolysis. The effect of acid type, acid-to-MCC ratio, reaction time, and numbers of high-pressure homogenization treatment on the resulted cellulose nanofibers and nanocrystals was examined. The study led to the following conclusions.

(1) An aggressive acid hydrolysis was shown to lead to rod-like cellulose nanocrystals with diameter about 10 nm and lengths in the range of 50–200 nm.

(2) Increased acid-to-MCC ratio and homogenization treatment passes further reduced the dimension of the nanocrystals produced. Weak acid hydrolysis was found to produce a network of cellulose nanofiber bundles having diameters in the range of 20–100 nm and lengths of a few thousands of nanometers.

(3) The high-pressure homogenization treatment helped separate the nanofiber bundles to form individual crystals.

(4) The thermal degradation behaviors indicated that the degradation of cellulose nanocrystals from sulfuric acid treatment started at a lower temperature and showed two remarkable pyrolysis processes. Cellulose nanofibers produced from hydrochloric acid hydrolysis had a much improved thermal stability.

Conflict of Interests

The authors declare that there is no conflict of interests regarding the publication of this paper.

Acknowledgments

This work is financially supported by the Louisiana Board of Regents OPT-IN grant program (LEQSF-EPS(2014)-OPT-IN-37) and by the Key Biomass Energy Laboratory of Henan Province, Henan, China. The authors would like to thank Dr. Haiyun Liu for her early involvement of the project.

References

[1] I. M. Saxena, K. Kudlicka, K. Okuda, and R. M. Brown, "Characterization of genes in the cellulose-synthesizing operon (acs operon) of Acetobacter xylinum: implications for cellulose crystallization," *Journal of Bacteriology*, vol. 176, no. 18, pp. 5735–5752, 1994.

[2] E.-L. Hult, P. T. Larsson, and T. Iversen, "Cellulose fibril aggregation—an inherent property of kraft pulps," *Polymer*, vol. 42, no. 8, pp. 3309–3314, 2001.

[3] M. M. de Souza Lima and R. Borsali, "Rodlike cellulose microcrystals: structure, properties, and applications," *Macromolecular Rapid Communications*, vol. 25, no. 7, pp. 771–787, 2004.

[4] D. Bondeson, A. Mathew, and K. Oksman, "Optimization of the isolation of nanocrystals from microcrystalline cellulose by acid hydrolysis," *Cellulose*, vol. 13, no. 2, pp. 171–180, 2006.

[5] S. Beck-Candanedo, M. Roman, and D. G. Gray, "Effect of reaction conditions on the properties and behavior of wood cellulose nanocrystal suspensions," *Biomacromolecules*, vol. 6, no. 2, pp. 1048–1054, 2005.

[6] Y. Shin, J. M. Blackwood, I.-T. Bae, B. W. Arey, and G. J. Exarhos, "Synthesis and stabilization of selenium nanoparticles on cellulose nanocrystal," *Materials Letters*, vol. 61, no. 21, pp. 4297–4300, 2007.

[7] O. A. Battista, "Hydrolysis and crystallization of cellulose," *Industrial & Engineering Chemistry*, vol. 42, no. 3, pp. 502–507, 1950.

[8] J. Araki, M. Wada, S. Kuga, and T. Okano, "Flow properties of microcrystalline cellulose suspension prepared by acid treatment of native cellulose," *Colloids and Surfaces A: Physicochemical and Engineering Aspects*, vol. 142, no. 1, pp. 75–82, 1998.

[9] M. Henriksson, G. Henriksson, L. A. Berglund, and T. Lindström, "An environmentally friendly method for enzyme-assisted preparation of microfibrillated cellulose (MFC) nanofibers," *European Polymer Journal*, vol. 43, no. 8, pp. 3434–3441, 2007.

[10] S. Janardhnan and M. M. Sain, "Isolation of microfibrils—an enzymatic approach," *BioResources*, vol. 1, no. 2, pp. 176–188, 2006.

[11] A. Turbak, F. Snyder, and K. Sandberg, "Microfibrillated cellulose, a new cellulose product: properties, uses, and commercial potential," *Journal of Applied Polymer Science*, vol. 37, pp. 815–827, 1983.

[12] F. W. Herrick, R. L. Casebier, J. K. Hamilton, and K. R. Sandberg, "Microfibrillated cellulose: morphology and accessibility," *Journal of Applied Polymer Science*, vol. 37, pp. 797–813, 1983.

[13] A. N. Nakagaito and H. Yano, "The effect of morphological changes from pulp fiber towards nano-scale fibrillated cellulose on the mechanical properties of high-strength plant fiber based composites," *Applied Physics A: Materials Science and Processing*, vol. 78, no. 4, pp. 547–552, 2004.

[14] M. Pääkko, M. Ankerfors, H. Kosonen et al., "Enzymatic hydrolysis combined with mechanical shearing and high-pressure homogenization for nanoscale cellulose fibrils and strong gels," *Biomacromolecules*, vol. 8, no. 6, pp. 1934–1941, 2007.

[15] J. Han, C. Zhou, A. D. French, G. Han, and Q. Wu, "Characterization of cellulose II nanoparticles regenerated from 1-butyl-3-methylimidazolium chloride," *Carbohydrate Polymers*, vol. 94, no. 2, pp. 773–781, 2013.

[16] H. Liu, D. Liu, F. Yao, and Q. Wu, "Fabrication and properties of transparent polymethylmethacrylate/cellulose nanocrystals composites," *Bioresource Technology*, vol. 101, no. 14, pp. 5685–5692, 2010.

[17] N. E. Marcovich, M. L. Auad, N. E. Bellesi, S. R. Nutt, and M. I. Aranguren, "Cellulose micro/nanocrystals reinforced polyurethane," *Journal of Materials Research*, vol. 21, no. 4, pp. 870–881, 2006.

[18] J. Han, C. Zhou, Y. Wu, F. Liu, and Q. Wu, "Self-assembling behavior of cellulose nanoparticles during freeze-drying: effect of suspension concentration, particle size, crystal structure, and surface charge," *Biomacromolecules*, vol. 14, no. 5, pp. 1529–1540, 2013.

[19] L. Jiang, E. Morelius, J. W. Zhang, and M. Wolcott, "Study of the poly(3-hydroxybutyrate-co-3-hydroxyvalerate)/cellulose nanowhisker composites prepared by solution casting and melt processing," *Journal of Composite Materials*, vol. 42, no. 24, pp. 2629–2645, 2008.

[20] N. Wang, E. Ding, and R. Cheng, "Thermal degradation behaviors of spherical cellulose nanocrystals with sulfate groups," *Polymer*, vol. 48, no. 12, pp. 3486–3493, 2007.

[21] H. Yu, Z. Qin, B. Liang, N. Liu, Z. Zhou, and L. Chen, "Facile extraction of thermally stable cellulose nanocrystals with a high yield of 93% through hydrochloric acid hydrolysis under hydrothermal conditions," *Journal of Materials Chemistry A*, vol. 1, no. 12, pp. 3938–3944, 2013.

[22] Y. Yue, C. Zhou, A. D. French et al., "Comparative properties of cellulose nano-crystals from native and mercerized cotton fibers," *Cellulose*, vol. 19, no. 4, pp. 1173–1187, 2012.

[23] K. Oksman, A. P. Mathew, D. Bondeson, and I. Kvien, "Manufacturing process of cellulose whiskers/polylactic acid nanocomposites," *Composites Science and Technology*, vol. 66, no. 15, pp. 2776–2784, 2006.